Modeling and Forecasting the Southern Oscillation: A Time-Domain Approach*

PAO-SHIN CHU

Department of Meteorology, University of Hawaii, Honolulu, HI 96822

RICHARD W. KATZ

Environmental and Societal Impacts Group, National Center for Atmospheric Research,† Boulder, CO 80307

(Manuscript received 13 September 1984; in final form 21 May 1985)

ABSTRACT

An index consisting of the difference of normalized sea level pressure departures between Tahiti and Darwin is used to represent the Southern Oscillation (SO) fluctuations. Using a time-domain approach, autoregressive-moving average (ARMA) processes are applied to model and predict this Southern Oscillation Index (SOI) on a monthly and seasonal basis. The ARMA process which is chosen to fit the monthly SOI expresses the index for the current month as a function of both the SOI one month and seven (or nine) months ago, as well as the current and previous month's random error. A purely autoregressive (AR) process is identified as representative of the seasonal SO fluctuations, with the SOI for the current season being derived from the index for the immediate past three seasons and a single random disturbance term for the current season. To allow for the phase locking of the SOI with the annual cycle, ARMA processes with seasonally varying coefficients are also considered.

As one example of how these models could be used, seasonal SO variations have been forecast. When SOI observations from 1935 through the summer of 1983 are employed, the seasonal model indicates forecasts of positive SOI from fall 1983 through fall 1984. Forecasts based only on SOI observations from 1935 through spring 1982 show a low predictive skill for the SOI values from summer 1982 through winter 1984, whereas one-season-ahead forecasts starting with summer 1982 agree reasonably well with the actual SOI observations. These examples help illustrate the degree to which the future behavior of the SOI is predictable on the basis of its past history alone.

1. Introduction

An increased interest in the study of the Southern Oscillation (SO) in recent years reflects the important socioeconomic implications of short-term climate variability (e.g., Glantz and Thompson, 1981). In a compact expression, the SO is mainly a large-scale phenomenon in which atmospheric masses are exchanged between centers in the Pacific and Indian Oceans (Walker and Bliss, 1932, 1937). More specifically, pressure variations near the eastern South Pacific subtropical high tend to vary more or less inversely with those in the Indonesian low pressure zone. Owing to this appearance of the standing wavelike pattern in the zonal direction across two southern oceans, the term SO was coined. Important meteorological variables which are indicative of the SO fluctuations are sea level pressure, sea surface and air temperature, wind, geopotential height, rainfall, and cloudiness. Climate variability in low as well as midlatitudes over both Northern and Southern Hemispheres is intimately related to the SO. The El Niño phenomenon, as manifested in the occasional warmings of the east equatorial Pacific Ocean, is also linked with the SO, and both events are labeled ENSO.

Fluctuations in the SO have been monitored in terms of several indices. Recently, these indices have been based on the difference between monthly mean sea level pressures at a pair of stations (Quinn and Burt, 1972; Trenberth, 1976, 1984; Horel and Wallace, 1981; Chen, 1982; Rasmusson and Carpenter, 1982). These stations are generally located near regions of the South Pacific high pressure center and the Indonesian low. The pairs of stations include Easter Island (27.2°S, 109.4°W)–Darwin (12.4°S, 130.9°E); Easter Island–Djarkarta (6.11°S, 106.5°E); Tahiti (17.5°S, 150°W)–Darwin; and Rapa (28°S, 144°W)–Darwin. In addition, Wright (1975) devised an index from a combination of several stations located in the SO regime. As noted by Trenberth (1976, 1984), extreme caution must be exercised in the selection of an appropriate index for further investigation. This is necessary because apparent temporal lead and lag linkages exist among several pairs of the stations aforementioned, and these oblique phase relationships may render the index questionable.

* Contribution 85-01, University of Hawaii, Department of Meteorology.

† The National Center for Atmospheric Research is sponsored by the National Science Foundation.

Moreover, missing observations and inhomogeneity at several stations present a further challenge to the construction of an index. Given these considerations, an index consisting of the pressure difference of Tahiti-minus-Darwin should be close to optimal, since pressure variations in Tahiti are approximately out of phase (180°) with those in Darwin (Chen, 1982; Trenberth, 1984). Furthermore, both stations have long-term complete observations since 1935. It is this particular SO index (SOI) that will be used throughout the paper.

The spectral characteristics of the SO, based on the Tahiti-minus-Darwin normalized index, have been explored by Trenberth (1976) and Chen (1982). A broad frequency band of the spectral peak is revealed in the range of 2–10 years. More recently, Trenberth (1984) studied the signal versus noise in the SO. Although some month to month persistence is apparent in the SOI, the monthly index does not behave like a red noise (or first-order autoregressive) process (Trenberth, 1984). This conclusion is supported by the slow decaying of the autocorrelation functions with increasing lags and negative values at higher lags.

Although the SO fluctuations cannot be simply described by a first-order autoregressive process, it remains interesting to see whether it would be possible to model, in a statistical sense, the SO variations. If so, what would be the optimal statistical model to describe the behavior of the SO fluctuations? Furthermore, to what extent can future values of the SOI be predicted from its past history alone based on this optimal model? The purpose of the current study thus focuses on the stochastic modeling and forecasting of the SO from a time-domain approach. Autoregressive-moving average (ARMA) processes, a class of models which allow for dependence over time of a more complex nature than that for a red noise process, will be applied to the monthly as well as seasonal SOI.

Section 2 reviews some basic properties of ARMA processes. Data source and treatment are described in Section 3. Modeling of the monthly and seasonal SOI and forecasting of the seasonal SOI are presented in Section 4. A summary and conclusions are found in Section 5.

2. Time series modeling and forecasting

a. Modeling

A parametric time series modeling approach is taken in this study. A stationary stochastic process X_t with mean zero is an ARMA(p; q) process if it can be expressed as:

$$X_t = \phi_1 X_{t-1} + \cdots + \phi_p X_{t-p} + a_t - \theta_1 a_{t-1} - \cdots - \theta_q a_{t-q}, \quad (1)$$

where the a_t constitute a white noise process consisting of a series of uncorrelated random variables, each of which has a Gaussian distribution with mean zero and variance σ_a^2. The ϕ and θ values are parameters related to an AR process and a moving average (MA) process, respectively, that need to be estimated. Equation (1) can be written simply as

$$\Phi(B)X_t = \Theta(B)a_t \quad (2)$$

where $\Phi(B)$ and $\Theta(B)$ are polynomials of degree p and q in B, and B is the backward shift operator, defined by $B^d X_t = X_{t-d}$.

To identify an appropriate ARMA process, examination of the autocorrelation and partial autocorrelation functions is most crucial. For example, in the case of a simple AR(1) process, the autocorrelation function (acf) decays exponentially to zero, whereas the partial autocorrelation function (pacf) cuts off after the first lag (Fig. 1). The behavior of the acf and pacf for an MA(1) process is exactly reversed to that for an AR(1) process. For an ARMA(1; 1) process, the acf and pacf are dominated by a mixture of damped exponential and/or damped sine waves starting from the first lag. When higher orders of p and q are involved in the mixed ARMA process, the behavior of the acf and pacf is more complicated. In particular, a model as simple as an AR(2) process can produce "pseudoperiodic" behavior (Box and Jenkins, 1976, p. 59), meaning that this approach can, if necessary, allow for the quasi-periodicities that the SOI has been claimed to possess. Methods for computing the theoretical autocorrelation function for a general ARMA process are given in Box

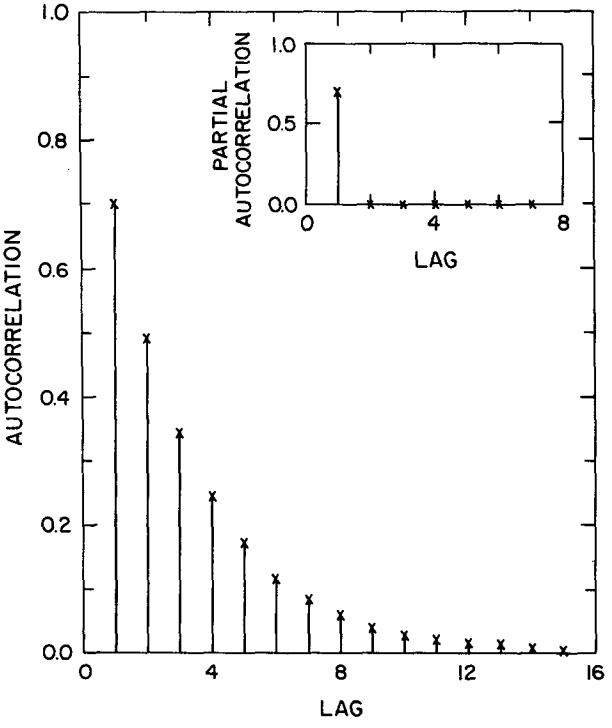

FIG. 1. Theoretical autocorrelation and partial autocorrelation functions for an AR(1) process, when $\phi_1 = 0.70$.

and Jenkins (1976, p. 75) and some specific examples are provided in the Appendix.

Constraints are ordinarily placed on the AR and MA parameters (ϕ and θ) so that the ARMA process will be stationary and invertible. *Stationarity* means that the joint distributions of the X are time invariant. Because of seasonal cycles, meteorological time series need to be normalized in order for this assumption to be reasonable. *Invertibility* means that the ARMA process has an equivalent representation as an infinite-order AR process, which is necessary for the model to be physically sensible. An AR(1) process is stationary if $|\phi_1| < 1$ and is, by definition, always invertible. In general, an ARMA process is stationary if the roots of the equation $\Phi(B) = 0$ all lie outside the unit circle and invertible if the roots of the equation $\Theta(B) = 0$ all lie outside the unit circle (Box and Jenkins, 1976, p. 74).

As a final step, the model should be checked diagnostically to reveal any inadequacies. If the selected model adequately fits the data, the residuals (i.e., estimators of the a_t) should be approximately serially uncorrelated. This property can be checked by examining the sample autocorrelations of the residuals.

In considering various stochastic models that are approximately representative of the data. One important factor is that the final model should contain as few parameters as possible. This parsimonious consideration in model building is important because simple models frequently offer plausible physical interpretation. In addition, overparameterization (i.e., higher values of p and q than necessary) may lead to unstable parameter estimates and thus result in less accurate forecasts. In practice, it is difficult to select objectively the appropriate orders of an ARMA process to represent the data. Katz and Skaggs (1981), Katz (1982), and Brown *et al.* (1984) have employed an automatic selection procedure to determine the orders of the process. This procedure, introduced by Schwarz (1978), is called the Bayesian Information Criterion (BIC). It is expressed mathematically as

$$\mathrm{BIC}(p; q) = N \ln\hat{\sigma}_a^2(p; q) + S \ln N, \qquad (3)$$

where $\hat{\sigma}_a^2(p; q)$ denotes an estimator of the variance σ_a^2 of the error terms (i.e., residual mean square) based on fitting an ARMA(p; q) process to the data, N the total number of observations, S the total number of parameters required to be estimated (e.g., $S = p + q + n$), and n is the total number of additional parameters [besides the $p + q$ parameters of the ARMA(p; q) process] that must be estimated. One estimator of σ_a^2 is

$$\hat{\sigma}_a^2(p; q) = [N - S]^{-1} \sum_{t=1}^{N} \hat{a}_t^2. \qquad (4)$$

Here the residual $\hat{a}_t$ is an estimate of the error term a_t. Since normalized departures involving the mean and standard deviation are used in the Tahiti and Darwin series, the value of n in the monthly data turns out to be 24 (12 estimated monthly means and 12 estimated standard deviations). Likewise, n is 8 for the seasonal SOI.

Looking back at (3), we note that the first term on the right-hand side represents the model performance and the second term is a penalty function for the S parameters that need to be estimated when an ARMA(p; q) process is fit to the data. As more parameters are brought into the model, the first term will usually decrease but the second term will necessarily increase. In general, a model with the minimum BIC value is preferred to others; however, this criterion should not be rigidly followed. Hannan (1980) has shown that selecting the orders p and q that minimize (3) leads to a consistent estimator of the true orders of an ARMA process. Alternatively, other model selection techniques, such as Akaike's information criterion (AIC) (Akaike, 1974) could be employed. The AIC involves the same model performance term as the BIC, but the penalty function term is of a somewhat different form.

b. *Forecasting*

Once an appropriate model has been obtained, forecasting can be made, say, at time origin t for lead time l. From (1), we can write the forecast $\hat{X}_t(l)$ in difference form as

$$\hat{X}_t(l) = \phi_1 X_{t+l-1} + \cdots + \phi_p X_{t+l-p} + a_{t+l} - \theta_1 a_{t+l-1} \cdots - \theta_q a_{t+l-q}. \qquad (5)$$

In (5), forecasted values are substituted for X values that have not yet been observed and error terms that have not yet been observed are set equal to zero.

It is also desirable to calculate the variance, $V(l)$ say, of the errors of l-step ahead forecasts, which is given by

$$\left.\begin{aligned} V(1) &= \sigma_a^2 \\ V(l) &= (1 + \sum_{j=1}^{l-1} \psi_j^2)\sigma_a^2, \quad l = 2, 3, \cdots \end{aligned}\right\}. \qquad (6)$$

Note that $\lim_{l\to\infty} V(l) = \sigma^2$, the variance of the process; i.e., the predictive skill of forecasts based on an ARMA process decreases to zero as the lag increases. The ψ weights in (6) can be obtained by equating coefficients of powers of B in

$$\Phi(B)(1 + \psi_1 B + \psi_2 B^2 + \cdots) = \Theta(B). \qquad (7)$$

With $\hat{X}_t(l)$ and $V(l)$ given, we can calculate the 100(1 $-$ α)% prediction limits for X_{t+l} as (Box and Jenkins, 1976, p. 137)

$$X_{t+l}(\pm) = \hat{X}_t(l) \pm Z_{\alpha/2}[V(l)]^{1/2}, \qquad (8)$$

where $Z_{\alpha/2}$ is the unit deviate exceeded by a proportion $\alpha/2$ of the Gaussian distribution. In practice, the ARMA parameter estimates (i.e., $\hat{\phi}$ and $\hat{\theta}$) are substituted for the unknown parameters in (5) to calculate

a forecast and in (7) to determine the ψ weights. This substitution makes the prediction limits only approximate, with the intervals being somewhat too short when the ARMA parameter estimates are based on a small sample size. Brown *et al.* (1984) includes an example of the calculation of these prediction intervals for the special case of an AR(2) process.

3. Data and processing

The monthly mean sea level pressure (SLP) observations at Tahiti and Darwin are obtained from the Monthly Climatic Data for the World (National Climatic Center, 1971–83) and World Weather Records (ESSA, 1941–70). Early data (1935–40) are provided by M.-C. Wu of the University of Wisconsin–Madison. The period of data used to develop the models runs from January 1935 through August 1983 without any missing observations. Since the annual cycle is apparent in the data, as noted by Trenberth (1984), it is imperative to remove this cycle before fitting ARMA processes so that the assumption of stationarity could be satisfied. Normalization is achieved by taking the difference between raw monthly mean data and the long-term monthly average, and then by dividing this departure by the standard deviation for each month at these two stations. The Tahiti-minus-Darwin difference in the corresponding month forms the monthly Southern Oscillation Index (584 values). Note that Trenberth (1984) has argued that this method of normalization is optimal. A similar index has been used at the Climate Analysis Center (CAC) of NOAA for operationally monitoring the SO. The quantitative value of the CAC's index differs somewhat, due to the normalization not being based on the identical sampling period.

In this study, seasonal mean values (194 observations) of the SOI are also used. For the seasonal SOI, winter is defined from December of the preceding year to February of the following year (e.g., winter of 1981 runs from December 1980 through February 1981, etc.). The raw, three consecutive monthly SLP data are averaged to produce a seasonal value for each station. In a way similar to the monthly data processing, normalization has been applied to each individual seasonal series and the Tahiti-minus-Darwin series form the seasonal SOI. This method of normalization implies that monthly and seasonal SOI time series both have mean zero. Histograms for the distributions of monthly and seasonal data are found to be approximately Gaussian. Due to the small number of yearly mean observations (48 values), no attempt has been made to model the yearly SOI.

4. Applications of stochastic models to the Southern Oscillation Index

a. *Modeling the monthly SOI*

Figure 2 shows a time series plot of the monthly SOI data, with rapid fluctuations about the mean value

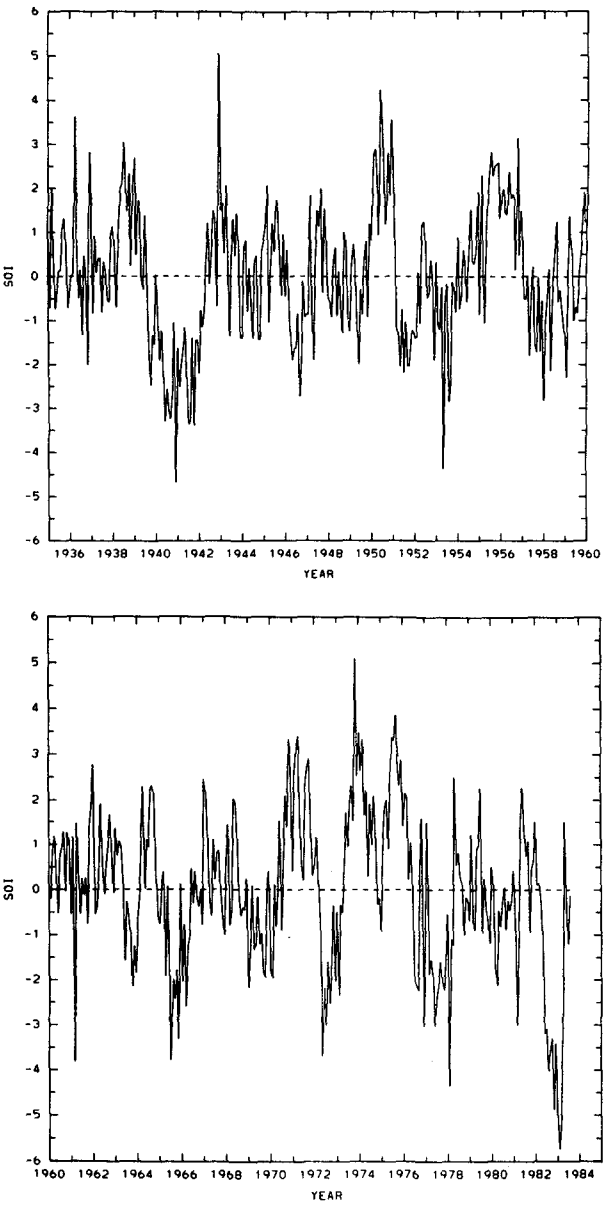

FIG. 2. Time series plot of the monthly SOI from January 1935 through August 1983.

(zero) being evident. Figure 3a shows the sample autocorrelation function of the monthly SOI up to 24 lags, revealing a generally damped exponential fall off, consistent with Trenberth's analysis (1984). In Fig. 3b, the sample partial autocorrelations exhibit a damped sine wave and are small after the first lag. From the general properties of ARMA processes discussed in the preceding section, the plausible candidates involve purely AR or mixed ARMA processes. The error variance $\hat{\sigma}_a^2$ and BIC value for seven preliminary monthly SOI models involving relatively small values of p and q, as well as for an uncorrelated process, are listed in the top part of Table 1. Among these candidate models, an ARMA(1; 1) process has the smallest BIC value.

TABLE 1. Estimated error variance $\hat{\sigma}_a^2$ and BIC value of ARMA models for monthly SOI time series.

		ARMA(p; q) models	
p	q	$\hat{\sigma}_a^2(p; q)$	BIC(p; q)
0	0*	2.789	751.9
1	0	1.683	463.4
2	0	1.591	436.8
1	1	1.546	420.0
1	2	1.548	427.2
3	0	1.539	423.8
2	1	1.550	427.9
4	0	1.533	434.2
		ARMA(1, p; q)	
p**	q	$\hat{\sigma}_a^2(1, p; q)$	BIC(1, p; q)
3	1	1.532	421.1
4	1	1.535	422.2
5	1	1.535	422.2
6	1	1.521	416.9
7	1	1.481	401.3
8	1	1.484	402.5
9	1	1.480	401.0
10	1	1.488	404.1
11	1	1.501	409.2
12	1	1.501	409.2

* Uncorrelated process.
** Single higher-order lag of AR process.

The theoretical autocorrelation function for this particular ARMA(1; 1) process (Box and Jenkins, 1976, p. 76) decreases toward zero at a geometric rate for higher lags (never becoming negative), unlike the sample autocorrelation function.

In an attempt to determine whether a model with a theoretical autocorrelation function in closer agreement with that for the monthly SOI time series can be found, more complex ARMA processes are also considered. In keeping with the goal of parsimony and the general characteristics of ARMA processes mentioned earlier, a single higher-order AR term (i.e., lag 3, 4, . . . , or 12) is added to the ARMA(1; 1) process. The error variance and BIC value for these ten additional models [denoted by ARMA(1, p; q)] are included in the bottom part of Table 1. The models involving the addition of a lag seven or nine AR term have the smallest error variance and BIC value. Because all of these additional models have three ARMA parameters, the BIC is not particularly useful for discriminating among them. Instead, the more stringent criterion is followed that the error variance be significantly reduced over that for the ARMA(1; 1) process, which is the case when either a lag seven or nine AR term is added (i.e., significant at the 1% level according to the partial F-test).

For simplicity, it is arbitrarily decided to adopt the model that involves the addition of the lag seven, rather than lag nine, AR term. Formally, this ARMA(1, 7; 1) is given by [as a special case of (1)]

$$X_t = \phi_1 X_{t-1} + \phi_7 X_{t-7} + a_t - \Theta_1 a_{t-1} \qquad (9)$$

where the parameter estimates are $\hat{\phi}_1 = 1.011$, $\hat{\phi}_7 = -0.115$, $\hat{\theta}_1 = 0.680$, and $\hat{\sigma}_a^2 = 1.481$ [or about a 47% reduction in the variance from that for an uncorrelated process; about a 12% reduction from that for an AR(1) process; and about a 4% reduction from that for an ARMA(1; 1) process (Table 1)]. The theoretical autocorrelation function for an ARMA(1, 7; 1) process with these particular parameter values is also included in Fig. 3a (see Appendix for a description of the method by which this function is calculated). Unlike the case of an ARMA(1; 1) process, this theoretical autocorrelation function starts taking on negative values at virtually the same lag as the sample autocorrelation function for the monthly SOI time series and shows close overall agreement. This model is further supported by the relatively small magnitudes and lack of patterns in the autocorrelations of the residuals (Fig. 4).

For this ARMA(1, 7; 1) process, we may regard the present value of the monthly SOI as a linear combination of the one month and seven months ago observations as well as some random shocks. In other words, the current month's SOI depends not only on the SOI one month and seven months ago, but also on a random noise term for the current month and the previous month's noise term. The complexity of the noise terms may be necessary to take into account some abrupt changes which occur occasionally in the monthly data. For example, a large positive index (+1.22) is revealed in February 1979, but moderate, negative values are observed in January (−0.68) and March (−0.72) of the same year.

Although the origin of the random noises in the monthly data is not clear, cold surge propagation during the winter season and the 40–50 day oscillation in tropical wind (Madden and Julian, 1971; Weickmann, 1983) appear to be important in perturbing the "normal" mode of operation of the SO. According to the International Monsoon Experiment (MONEX) management center, there were eight active cold surges identified over East Asia during the period 1 December 1978 to 28 February 1979. Out of the eight cases, only one surge occurred in central China near the end of January which was regarded as moderate/strong (Shaffer *et al.*, 1984). Since a surge with moderate strength is effective in transporting lower-tropospheric mass from central China to Borneo within a few days during the northern winter (Chu and Park, 1984), the relatively strong surge reported on 29 January in Hong Kong may penetrate further southward to the Indonesian/Australasian low pressure region by early February. As a consequence, the mass field in the Indonesian region would be adjusted instantly by this external forcing. This adjustment should be reflected in the Darwin normalized SLP, as seen by the change from a small negative value in January to a small positive value in February. In the meantime, the Tahiti normalized SLP, which is influenced by the strength and position of the South Pacific anticyclone, also under-

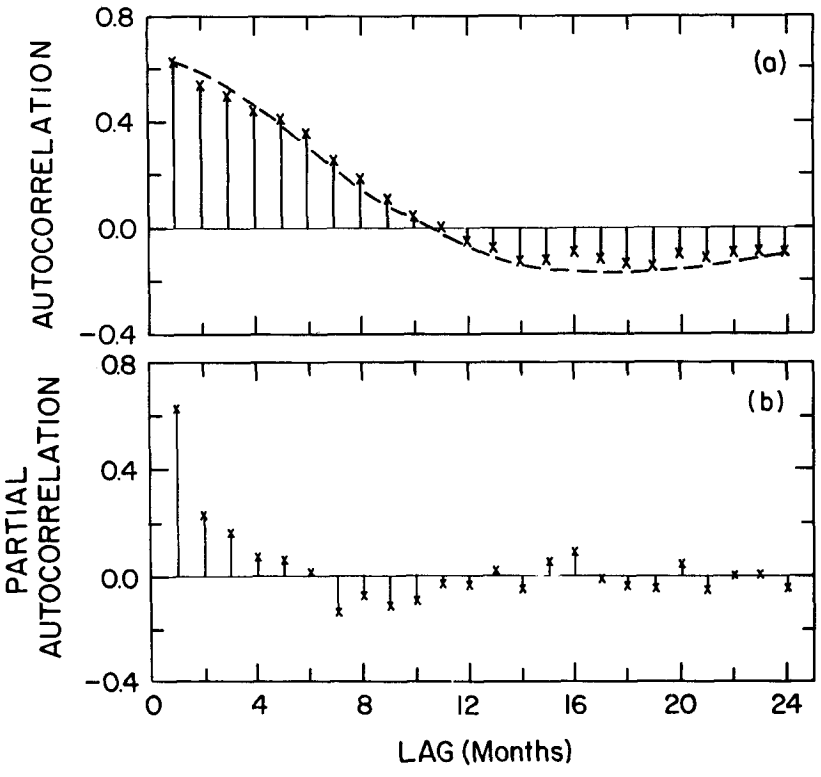

FIG. 3. (a) Sample autocorrelation function of the monthly SOI and theoretical autocorrelation function (broken line) for ARMA (1, 7; 1) process. (b) Sample partial autocorrelation function of the monthly SOI: January 1935 through August 1983.

went a similar but rather large change. Recent operational observations indicate that anomalously tropical convection associated with the 40–50 day oscillation did propagate eastward from the western Indian Ocean to the equatorial central Pacific (Climate Analysis Center, 1985). It may be due to these reasons that the monthly SOI varied abruptly from January (−0.68) to February (+1.22). In view of these observations, it is

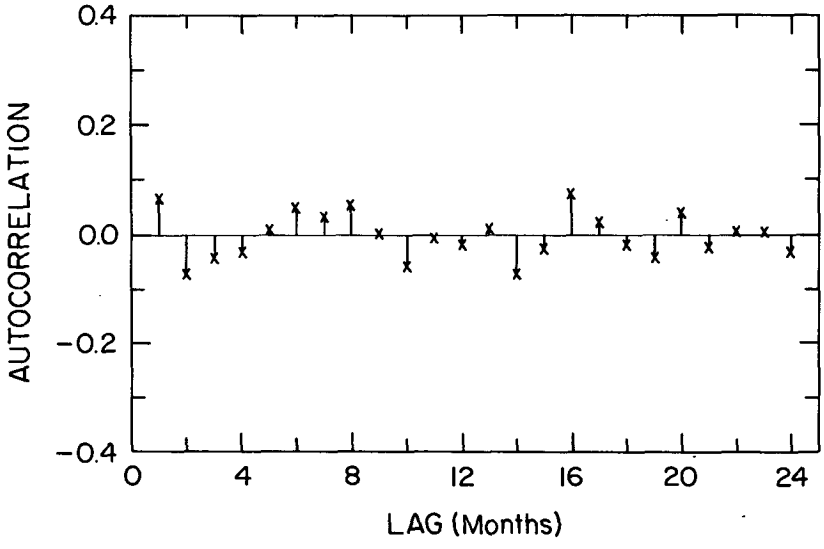

FIG. 4. Sample autocorrelation function of ARMA (1, 7; 1) residuals for the monthly SOI: January 1935 through August 1983.

possible that strong midlatitude forcing, as manifested in a cold surge, together with the eastward movement of tropical convection, would perturb the large-scale mass circulation in the SO regime on a short time basis. Of course, the pressure variations in Darwin may also be modulated by other factors such as tropical cyclones.

b. *Modeling the seasonal SOI*

Figure 5 displays the temporal variations of the seasonal SOI, with the pattern being somewhat smoother than the corresponding plot of monthly SOI (Fig. 2). While an oscillatory feature is present throughout the entire series, large negative anomalies in recent years are particularly conspicuous. The four recent seasons beginning with summer 1982 through spring 1983 are marked by significantly negative values unprecedented since 1935. A seasonal climatic summary related to these extraordinary anomalies is described by Wagner (1983), Krueger (1983), Quiroz (1983), and Chen (1983).

The sample autocorrelations of the seasonal SOI tail off toward zero (Fig. 6a) and the sample partial autocorrelations are small after the first three lags (Fig. 6b). This behavior suggests that the seasonal time series might be described by purely AR or mixed ARMA processes. The error variance and BIC value for eight preliminary seasonal SOI models, as well as for an uncorrelated process, are listed in Table 2. An AR(3) process appears to be the model with the smallest sum of orders ($p + q = 3$) that has relatively low error variance. In particular, an AR(3) process exhibits the lowest BIC value. This model is of the form [as a special case of (1)]

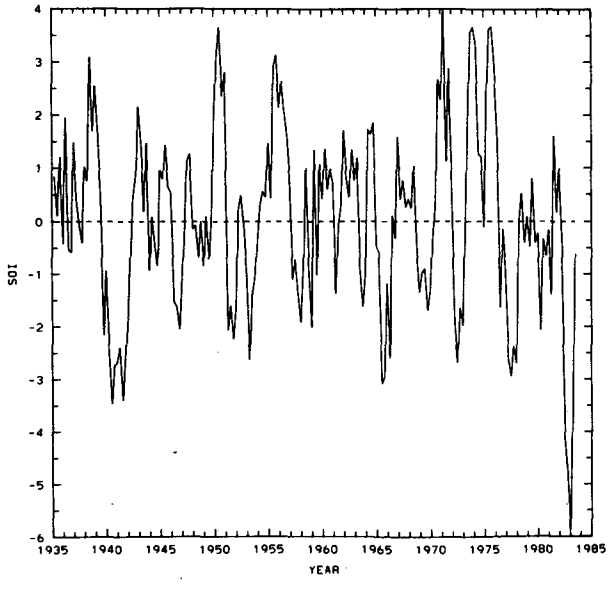

FIG. 5. Time series plot of the seasonal SOI from spring 1935 to summer 1983.

$$X_t = \phi_1 X_{t-1} + \phi_2 X_{t-2} + \phi_3 X_{t-3} + a_t, \qquad (10)$$

where the parameter estimates are $\hat{\phi}_1 = 0.6885$, $\hat{\phi}_2 = 0.2460$, $\hat{\phi}_3 = -0.3497$, and $\hat{\sigma}_a^2 = 1.505$ [or about a 54% reduction in the variance from that for an uncorrelated process and about an 11% reduction from that for an AR(1) process (Table 2)]. The pattern of the sample autocorrelations for the AR (3) residuals appears to be random and all autocorrelations are relatively small (Fig. 7). The theoretical autocorrelation function for an AR(3) process (Box and Jenkins, 1976, p. 54) with these particular values is also included in Fig. 6a (see Appendix for the method of calculation). Note that the theoretical autocorrelation function drops below zero at lag four (like the sample autocorrelation function) and then continues a damped oscillation about zero. When higher-order AR terms are added to the AR(3) model, the fit is not significantly improved. Perhaps this result is attributable to the fact that a lag three AR term in the seasonal model corresponds to roughly the same time scale as a lag seven (or lag nine) AR term in the monthly model, and thus the AR(3) seasonal model is roughly consistent with an ARMA(1, 7; 1) [or ARMA(1, 9; 1)] monthly model.

This selected AR(3) model implies that the current value of a seasonal SOI is a finite, linear aggregate of three preceding seasonal values and a white noise term. Since the seasonal data are smoother than the monthly data due to the averaging effect, intraseasonal persistence might be more dominant than the noise in the seasonal SOI. We may interpret this model physically as follows. Presumably, the SO is a large-scale phenomenon in close connection with sea surface temperature anomalies in the tropics involving heat transfer between the ocean and atmosphere, trade wind stress relaxation and, possibly, Kelvin wave propagation from the west equatorial Pacific to the Peruvian coast (Wyrtki, 1975). The anomalous thermal forcing of the tropical oceans in modulating the SO is a slow but steady process. Horel and Wallace (1981) and Rasmusson and Carpenter (1982) showed that the lifetime of a typical warm episode associated with the SO in the equatorial Pacific can last more than one year. The need to consider three preceding seasonal SOI in the seasonal model may be attributed to the large thermal inertia in the oceans and its gradual change in time.

One statistical explanation of why a moving average term appears in the selected model for the monthly SOI time series, but not in the model for the seasonal SOI, involves the presence of measurement error. It can be shown that, if an underlying AR(p) process is subject to measurement error, then the observed process is ARMA(p; p) (Box and Jenkins, 1976, p. 121); i.e., the presence of measurement error introduces p moving average terms. This explanation is relevant because the single stations, Darwin and Tahiti, are employed to represent pressure patterns over large areas, so that some measurement error is surely present. On

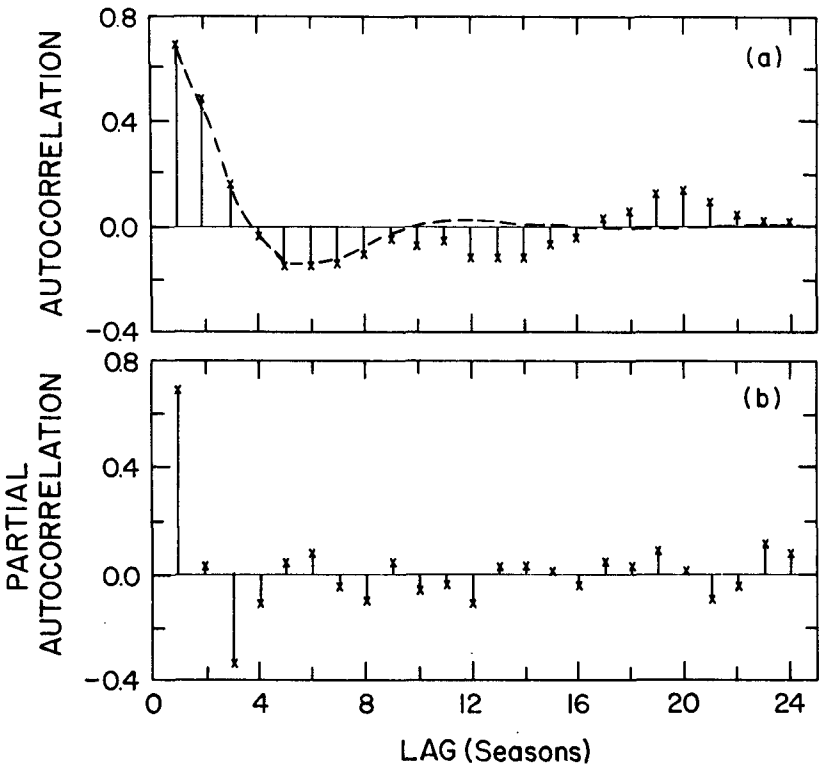

FIG. 6. (a) Sample autocorrelation function of the seasonal SOI and the theoretical autocorrelation (broken line) for AR(3) process. (b) Sample partial autocorrelation function of the seasonal SOI: spring 1935 through summer 1983.

the other hand, such measurement error should be smaller, and perhaps have negligible effects, when the SOI is smoothed from monthly to seasonal values.

Although the SOI is normalized, this procedure only removes seasonal cycles in the mean and standard deviation and ignores any seasonal patterns in the autocorrelation function [or, equivalently, in the ARMA parameters (ϕ and θ)]. On the other hand, there is evidence that the SOI is phase locked to the annual cycle (e.g., Philander, 1983), and thus the degree of its persistence does vary seasonally. To investigate further this issue, an AR(3) process with seasonally varying parameters is fit to the seasonal SOI time series. This model can be expressed [as a generalization of (10)] as

$$X_t = \phi_1(t)X_{t-1} + \phi_2(t)X_{t-2} + \phi_3(t)X_{t-3} + a_t \quad (11)$$

where variance $(a_t) = \sigma_a^2(t)$ and these parameters vary periodically; i.e.,

$$\phi_i(t) = \phi_i(t-4), \quad i = 1, 2, 3;$$
$$\sigma_a^2(t) = \sigma_a^2(t-4). \quad (12)$$

The specific parameter estimates are given in Table 3. It is evident that there is a substantial degree of seasonal variation in the AR parameters, although the general structure of the AR(3) processes is similar with the coefficients for the first two lags always being positive and those for the third lag always being negative. The one-season-ahead forecasting skill, as measured by the estimated error variances which vary from a minimum of 1.037 (70% reduction in variance) when making one-season-ahead predictions of fall SOI to a maximum of 2.207 (44% reduction in variance) when making one-season-ahead predictions of summer SOI, averages out to about 1.638 or roughly the same as the error variance for the AR(3) model (10) that does not vary seasonally (i.e., 1.505).

TABLE 2. Estimated error variance $\hat{\sigma}_a^2$ and BIC value of ARMA(p; q) models for the seasonal SOI time series.

p	q	$\hat{\sigma}_a^2(p; q)$	BIC(p; q)
0	0*	3.279	272.5
1	0	1.689	149.1
2	0	1.696	155.2
1	1	1.710	156.6
3	0	1.505	137.3
2	1	1.662	156.6
1	2	1.537	141.3
4	0	1.484	139.8
5	0	1.468	143.0

* Uncorrelated process.

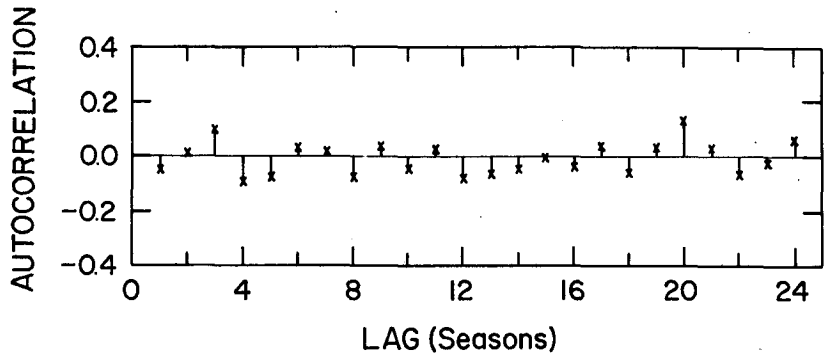

FIG. 7. Sample autocorrelation function of AR(3) residuals for the seasonal SOI: spring 1935 through summer 1983.

c. *Forecasting the seasonal SOI since fall 1983*

A useful way to interpret the properties of a given ARMA model is to examine how it performs in forecasting future values of the time series analyzed. Although techniques that include the use of other meteorological or oceanographical variables would certainly be expected to produce more accurate forecasts of ENSO events (e.g., Barnett, 1984), it is still of interest to determine how well an individual time series can be predicted on the basis of its own past history alone. To illustrate the use of an ARMA process for forecasting, the seasonal model outlined in the preceding subsection will be used to forecast seasonal SOI from fall 1983 through fall 1984. Note that this predicted period does not fall into the time interval which is used to construct the seasonal model (i.e., spring 1935 through summer 1983), thus making these "genuine" predictions.

In Fig. 8, the predicted values of the SOI obtained using (5) and the 95% prediction limits are shown, together with the observed SOI for fall 1983 and winter 1984. (The original monthly mean data from September 1983 through February 1984 for Tahiti and Darwin were obtained through the courtesy of W. H. Quinn.) The prediction limits are interpreted as follows: Given the information available at the starting point t (summer 1983), there is a 95% probability that the limits will contain the actual value of X_{t+l}; note that the width of the prediction intervals increases until lag four and then is roughly constant beyond that point, indicating little or no forecasting skill four or more seasons in advance. Figure 8 shows that the forecast and observed

TABLE 3. Parameter estimates for AR(3) model with seasonally varying parameters of seasonal SOI time series.

Parameter estimates	SOI predictand			
	Spring (t = 1)	Summer (t = 2)	Fall (t = 3)	Winter (t = 4)
$\hat{\phi}_1(t)$	0.5268	0.7832	0.8554	0.7736
$\hat{\phi}_2(t)$	0.1158	0.2568	0.1700	0.1971
$\hat{\phi}_3(t)$	−0.2011	−0.3816	−0.0674	−0.1808
$\hat{\sigma}_a^2(t)$	2.117	2.207	1.037	1.191
R^{2*}	0.30	0.44	0.70	0.63

* Proportionate reduction in variance from an uncorrelated process.

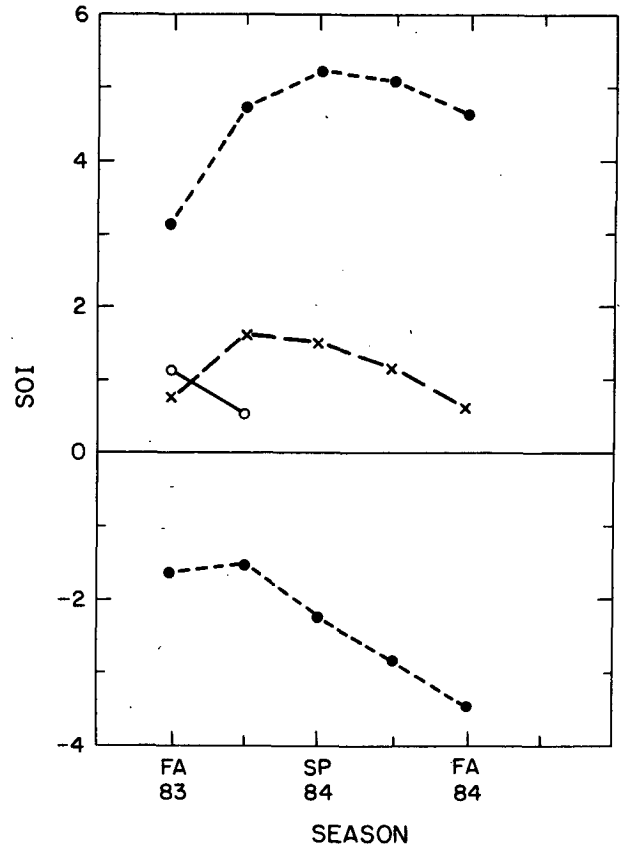

FIG. 8. Time series plots of forecast (long broken line) and observed (solid line) values of the seasonal SOI from fall 1983 (FA 83) through fall 1984 (FA 84). The forecasts are based on SOI observations through summer 1983. The 95% prediction limits for the forecast values are shown by short broken lines. Period of the analyzed model is spring 1935 through summer 1983.

values are both positive since fall 1983, although some slight differences in magnitude are found between the two series. The negative SOI observed during the period from spring 1982 through summer 1983 in Fig. 5, together with the successive positive values in Fig. 8, reflect a shift in the atmospheric masses across the two Southern oceans in recent years.

d. Forecasting the seasonal SOI since Summer 1982

In this subsection, we perform seasonal forecasts with a model based on a shorter record length. The period used to fit the model is spring 1935 to spring 1982, and we refer to this particular data set as SDS. Our particular interest is to see whether the "extreme" anomalies that occurred between summer 1982 and spring 1983 are predictable. The ARMA model is fit to the SDS, instead of the full data set, to again make these bona fide predictions.

A comparison of the sample autocorrelations and the sample partial autocorrelations for the SDS (figure not shown) with Fig. 6 indicates that the behavior of the acf and pacf of the SDS is virtually the same as that for the AR(3) model using the entire record length. These results suggest that even excluding the large anomalies aforementioned, the AR(3) process would still appear to be optimal. It is further supported by the small sample autocorrelations of the residuals (not shown). Accordingly, the estimated parameters of the model based on this SDS are $\hat{\phi}_1 = 0.6388$, $\hat{\phi}_2 = 0.2765$, $\hat{\phi}_3 = -0.3264$, and $\hat{\sigma}_a^2 = 1.371$. Since the "extreme" anomalies are not included in the SDS, this AR(3) process has, as expected, a somewhat smaller estimated error variance than the previous seasonal model (Section 4b).

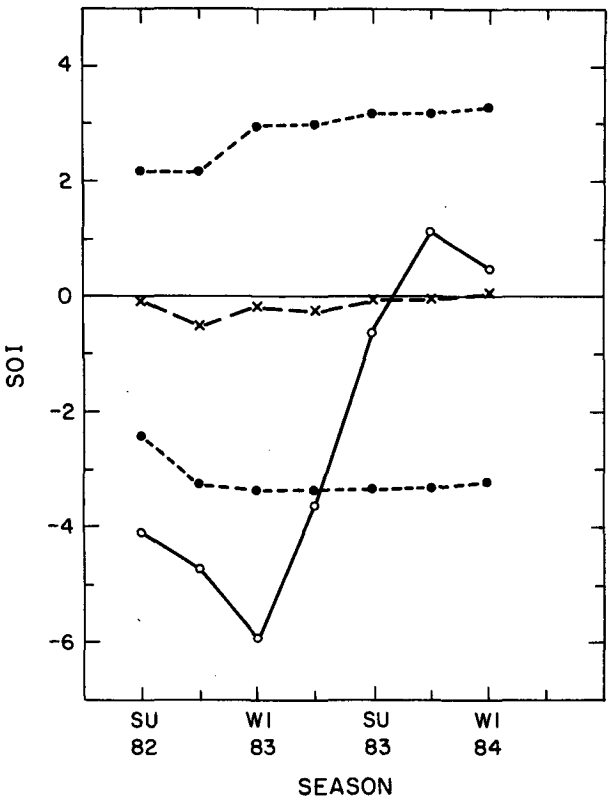

FIG. 9. As in Fig. 8, but for summer 1982 (SU 82) through winter 1984 (WI 84). The forecasts are based on observations through spring 1982. The 95% prediction limits for the forecast values are shown by short broken lines. Period of the analyzed model is spring 1935 through spring 1982.

Figure 9, derived from (5) and (8), displays the forecast values and 95% prediction intervals of the seasonal SOI, starting from summer 1982 based on observations through spring 1982, along with the actual observations. Although the SOI predictions are mainly negative, in accordance with the observations, a large discrepancy in magnitude is noted between these two series during the "extreme" seasons. An unusual seasonal evolution from spring (−0.47) to summer (−4.08) 1982 accounts for the large forecast errors in summer 1982 and the subsequent three seasons.

Since the large anomalies occurring in summer 1982 were unprecedented from 1935 onwards and since the prediction error increases as the lag l increases, it is not unexpected that such forecasts show little success. Alternatively, one-season-ahead forecasts at various time origins could be considered. Specifically, by means of (5), a forecast for summer 1982 can be produced using SOI observations through spring 1982; then a forecast for fall 1982 can be produced using SOI observations through summer 1982, and so on.

Figure 10 displays the one-season-ahead forecasts and 95% prediction intervals along with the actual observations from summer 1982 through winter 1984. Note that, because the forecasts in Fig. 10 are all for only one season in advance, the widths of the prediction intervals are smaller than those in Fig. 9 (other than those for summer 1982 which are, of course, identical in both figures). With the exception of summer 1982, a close correspondence between these two series is readily seen, both in the direction of variation and in magnitude. In summary, because of the peculiar seasonal evolution of general circulation anomalies from spring to summer 1982 which then persisted for the subsequent three seasons, the one-season-ahead forecasts (Fig. 10) of the SO variations are necessarily more accurate than the forecast for more than one season in advance (Fig. 9).

The questions arise as to whether the AR(3) model produces forecasts that are any more accurate than a simpler AR(1) model and as to whether the seasonally varying AR(3) model would produce even more accurate forecasts. For the same case of the one-step ahead forecasts based on the AR(3) model (Fig. 10), forecasts are also produced using AR(1) and AR(5) models. All three sets of forecasts are listed in Table 4, along with

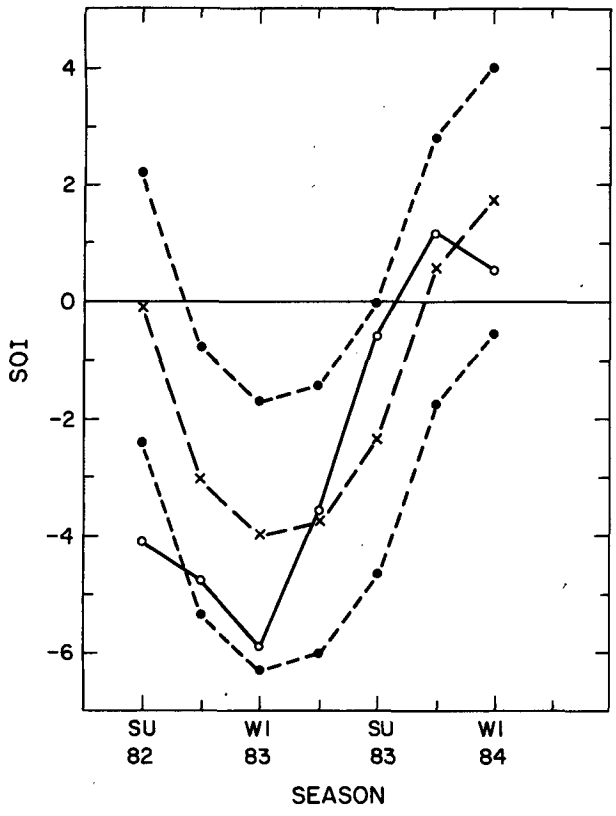

FIG. 10. Time series plots of one-season-ahead forecast (long broken line) and observed (solid line) values of the seasonal SOI from summer 1982 (SU 82) through winter 1984 (WI 84). The 95% prediction limits for the forecast values are shown by short broken lines. Period of the analyzed model is spring 1935 through spring 1982.

the root-mean-square error as a measure of the overall forecast accuracy. For this limited set of cases, the AR(3) model evidently produces forecasts that are slightly more accurate than those produced by the other two models. If the seasonally varying AR(3) model (11) were employed instead, the major difference is that the widths of the prediction intervals would vary with the season, making the actual confidence levels more nearly equal to the stated values.

5. Summary and conclusions

Fluctuations in the SO are monitored by the Tahiti-minus-Darwin normalized sea level pressure index, which covers the period since January 1935. A time-domain approach is applied to model the long-term SO variations on a monthly and seasonal basis. A potential class of models is first suggested and parameters of each possible model are estimated. Diagnostic checking of model adequacies is made. To help identify the appropriate model, an objective model selection procedure is used which is based on the principle of parsimony in model building approach.

It is found that the monthly SOI can be adequately modeled by a mixed autoregressive-moving average process with lag one and seven (or nine) AR terms and lag one MA term. For this particular process, the current state of the SOI can be derived from its immediate past state and its state seven (or nine) months ago plus a random disturbance and its immediate past shock. Strong midlatitude forcing as induced by the cold surge during winter season, together with the tropical 40–50 day oscillation, may perturb the "normal" behavior of the SO. As a result, the monthly index is occasionally contaminated by some transient circulation features which are not inherent in the large scale SO.

For the seasonal data, an AR(3) process is found to be the most adequate time series model. For this model, the current value of the SOI can be represented in terms of its three immediate past values and a noise term. The rather long carry-over effect (three seasons) is suggestive of a pronounced signal reflected in the seasonal data (Trenberth, 1984). Previous studies indicate that the lifetime of an anomalous warm sea surface temperature in the equatorial Pacific associated with the SO may last more than one year. This slow change in thermal forcing, together with large thermal inertia in the tropical oceans, offers an explanation for this long memory over at least three seasons. In this regard, it turns out that the noise contributes slightly less to the SO fluctuations on a seasonal basis than it does on a monthly basis.

Forecasting of the seasonal SO variations has been made using the spring 1935 through summer 1983 and spring 1935 through spring 1982 data sets. For the first data set, forecasts of the seasonal SOI from fall 1983 to fall 1984 are made based on SOI observations through summer 1983. The forecast values of the seasonal SOI are marked by positive values, in accordance with the recent observations for fall 1983 and winter 1984 (see Fig. 8). For the second data set, two types of forecasts are made to obtain values from summer 1982 through winter 1984. The forecasts based on SOI observations through spring 1982 show a large discrep-

TABLE 4. One-season-ahead forecasts for several AR models and observed SOI from summer 1982 through winter 1984.

Season	Forecast SOI AR(1)	Forecast SOI AR(3)	Forecast SOI AR(5)	Observed SOI
Summer 1982	−0.312	−0.082	−0.183	−4.08
Fall 1982	−2.709	−3.059	−2.912	−4.73
Winter 1983	−3.141	−3.996	−4.054	−5.88
Spring 1983	−3.904	−3.732	−4.191	−3.57
Summer 1983	−2.371	−2.362	−2.303	−0.62
Fall 1983	−0.412	0.536	0.582	1.17
Winter 1984	0.777	1.741	2.109	0.53
Root-mean-square error	2.122	1.973	1.996	

ancy in magnitude compared to the actual observations during the "extreme" seasons, although the direction of variation is in line with the actual observations (see Fig. 9). This discrepancy resulted from the extraordinarily abrupt seasonal variations of general circulation anomalies from spring to summer 1982. On the other hand, the one-season-ahead forecast values are in reasonable agreement with the observed anomalies (see Fig. 10 and Table 4).

Besides their use as a forecasting tool, these ARMA models for the SOI have other potential uses. For instance, the modeling of the autocorrelation structure of the SOI can aid in developing rigorous statistical tests of whether teleconnections are actually present between the SOI and other atmospheric variables. The ARMA models can also be used to produce simulated time series of the SOI. Such simulations might aid in studying the properties of statistical procedures that are applied to SOI data (e.g., teleconnections studies).

Acknowledgments. We thank B. Brown for her comments and help in drafting figures, and the editor, Dr. Kevin E. Trenberth, and the reviewers for suggestions that led to improvements in the manuscript. Discussions with C. Ramage and S. Esbensen were helpful. A portion of this research was supported jointly by the Division of Atmospheric Sciences of the National Science Foundation under Grant ATM-8209713 to the Department of Atmospheric Sciences at Oregon State University and by the National Oceanic and Atmospheric Administration under Contract NA80RAH00002 to JIMAR at the University of Hawaii.

APPENDIX

Calculation of Theoretical Autocorrelation Function

ARMA(1, 7; 1) process

Using the general recursive relationship for the theoretical autocovariance function of an ARMA(p; q) process (Box and Jenkins, 1976, p. 75), we note that the kth-order autocovariance coefficient γ_k for an ARMA(1, 7; 1) process is given by

$$\gamma_0 = \phi_1\gamma_1 + \phi_7\gamma_7 + [1 - \theta_1(\phi_1 - \theta_1)]\sigma_a^2, \quad \text{(A1)}$$

$$\gamma_1 = \phi_1\gamma_0 + \phi_7\gamma_6 - \theta_1\sigma_a^2, \quad \text{(A2)}$$

$$\gamma_k = \phi_1\gamma_{k-1} + \phi_7\gamma_{k-7}, \quad k = 2, 3, \cdots, 7. \quad \text{(A3)}$$

Equations (A1), (A2), and (A3) constitute a system of eight equations that can be solved for the eight unknowns $\gamma_0, \gamma_1, \ldots, \gamma_7$. Then the theoretical kth-order autocorrelation coefficient ρ_k for an ARMA(1, 7; 1) process is determined by

$$\rho_k = \gamma_k/\gamma_0, \quad k = 1, 2, \cdots, 7, \quad \text{(A4)}$$

$$\rho_k = \phi_1\rho_{k-1} + \phi_7\rho_{k-7}, \quad k = 8, 9, \cdots. \quad \text{(A5)}$$

AR(3) process

Using the general recursive relationship for the theoretical autocorrelation function of an AR(p) process (Box and Jenkins, 1976, p. 54), we note

$$\rho_k = \phi_1\rho_{k-1} + \phi_2\rho_{k-2} + \phi_3\rho_{k-3}, \quad k = 4, 5, \cdots, \quad \text{(A6)}$$

with ρ_1, ρ_2, and ρ_3 being set equal to the corresponding sample autocorrelation coefficients if the so-called Yule-Walker recursion is employed to estimate the AR parameters.

REFERENCES

Akaike, H., 1974: A new look at the statistical model identification. *IEEE Trans. Auto. Control,* **19,** 716–723.

Barnett, T. P., 1984: Prediction of the El Niño of 1982–1983. *Mon. Wea. Rev.,* **112,** 1403–1407.

Box, G. E. P., and G. M. Jenkins, 1976: *Time Series Analysis: Forecasting and Control* (rev.), Holden-Day, 575 pp.

Brown, B. G., R. W. Katz and A. H. Murphy, 1984: Time series models to simulate and forecast wind speed and wind power. *J. Climate Appl. Meteor.,* **23,** 1184–1195.

Chen, W. Y., 1982: Assessment of Southern Oscillation sea-level pressure indices. *Mon. Wea. Rev.,* **110,** 800–807.

——, 1983: The climate of spring 1983—A season with persistent global anomalies associated with El Niño. *Mon. Wea. Rev.,* **111,** 2371–2384.

Chu, P.-S., and S.-U. Park, 1984: Regional circulation characteristics associated with a cold surge event over East Asia during Winter MONEX. *Mon. Wea. Rev.,* **112,** 955–965.

Climate Analysis Center, 1985: Climate Diagnostics Bulletin, January 1985 (Available from NOAA/NWS Climate Analysis Center, National Meteorological Center, Washington, D.C. 20233).

Environmental Science Service Administration, U.S. Weather Bureau, 1941–70: World weather records, 1941–70. Washington, DC, 20402.

Glantz, M. H., and J. D. Thompson, Eds., 1981: *Resource Management and Environmental Uncertainty: Lessons from Coastal Upwelling Fisheries,* Wiley, 491 pp.

Hannan, E. J., 1980: The estimation of the order of an ARMA process. *Ann. Statist.,* **8,** 1071–1081.

Horel, J. D., and J. M. Wallace, 1981: Planetary scale atmospheric phenomena associated with the Southern Oscillations. *Mon. Wea. Rev.,* **109,** 813–829.

Katz, R. W., 1982: Statistical evaluation of climate experiments with general circulation models: A parametric time series modeling approach. *J. Atmos. Sci.,* **39,** 1446–1455.

——, and R. H. Skaggs, 1981: On the use of autoregressive-moving average processes to model meteorological time series. *Mon. Wea. Rev.,* **109,** 479–484.

Krueger, A. F., 1983: The climate of Autumn 1982—With a discussion of the major tropical Pacific anomaly. *Mon. Wea. Rev.,* **111,** 1103–1118.

Madden, R. A., and P. R. Julian, 1971: Detection of a 40–50 day oscillation in the zonal wind in the tropical Pacific. *J. Atmos. Sci.,* **28,** 702–708.

National Climatic Center, 1971–83: Monthly climatic data for the world, 1971–83. Asheville, NC 28801.

Philander, S. G. H., 1983: El Niño Southern Oscillation phenomena. *Nature,* **302,** 295–301.

Quinn, W. H., and W. V. Burt, 1972: Use of the Southern Oscillation in weather prediction. *J. Appl. Meteor.*, **11,** 616–628.

Quiroz, R. S., 1983: The climate of the El Niño winter of 1982–83—A season of extraordinary climatic anomalies. *Mon. Wea. Rev.*, **111,** 1685–1706.

Rasmusson, E. M., and T. H. Carpenter, 1982: Variations in tropical sea surface temperature and surface wind fields associated with the Southern Oscillation/El Niño. *Mon. Wea. Rev.*, **110,** 354–384.

Schwarz, G., 1978: Estimating the dimension of a model. *Ann. Statist.*, **6,** 461–464.

Shaffer, A. R., C.-P. Chang and R. L. Elsberry, 1984: Long wave forcing of equatorial penetrating winter monsoon cold surges. *Proc. 15th Conf. on Hurricanes and Tropical Meteorology,* Miami, Amer. Meteor. Soc., 427–432.

Trenberth, K. E., 1976: Spatial and temporal variations of the Southern Oscillation. *Quart. J. Roy. Meteor. Soc.*, **102,** 639–653.

———, 1984: Signal versus noise in the Southern Oscillation. *Mon. Wea. Rev.*, **112,** 326–332.

Wagner, A. J., 1983: A season with increasingly anomalous circulation over the equatorial Pacific Ocean. *Mon. Wea. Rev.*, **111,** 590–601.

Walker, G. T., and E. W. Bliss, 1932: World Weather V. *Mem. Roy. Meteor. Soc.*, **4,** 53–84.

——, and ——, 1937: World Weather IV. *Mem. Roy. Meteor. Soc.*, **4,** 119–139.

Weickmann, K. M., 1983: Intraseasonal circulation and outgoing longwave radiation modes during Northern Hemisphere winter. *Mon. Wea. Rev.*, **111,** 1838–1858.

Wright, P. B., 1975: An index of the Southern Oscillation. *Climate Res. Unit Rep. CRU RP4,* Norwich, U.K., 22 pp.

Wyrtki, K., 1975: El Niño—the dynamic response of the equatorial Pacific Ocean to atmospheric forcing. *J. Phys. Oceanogr.*, **5,** 572–584.